JOURNAL OF PURE APPLIED AND INDUSTRIAL PHYSICS
An International Open Free Access, Peer Reviewed Research Journal
www.physics-journal.org

ISSN 0976-5727 (Print)
ISSN 2319-8133 (Online)
Abbr:J. Pure Appl. & Ind. Phys.
2014, Vol.4(3): Pg.111-118

Structural, Dielectric Relaxation and Electrical Characterization of $CaNb_2O_6$ Phase Pure Material

K. N. Singh[*], A. K. Srivastava, Umesh Kushwaha and [1]P. K. Bajpai

Department of Physics,
Dr. C.V. Raman University Bilaspur, C. G., INDIA.
[1]Advance Material Research Laboratory,
Department of Pure & Applied Physics
Guru Ghasidas University, Bilaspur, C. G., INDIA.

(Received on: May 05, 2014)

ABSTRACT

Controlling the cooling rate during calcinations and sintering, have prepared pure columbite like phase of $CaNb_2O_6$ by simple solid state reaction route. The samples are characterized by X-ray diffraction analysis and scanning electron microscopy. The X-ray diffraction shows pure columbite like phase with orthorhombic structure. The lattice constants were obtained a=5.772 Å, b=14.9897Å, c=5.2375 Å. Density of material is found 4.36 g_m/cm^3 (92% of theoretical density) in the sample sintered at 1250^0C. Detailed studies of ε' and ε'' shows that the compound exhibits dielectric anomaly at 112^0C. Temperature dependent relative permittivity ε' indicates that the dielectric polarization has a relaxation type behavior. Frequency dependence of the real (ε') and imaginary (ε'') part of the dielectric permittivity shows typical characteristic of ferroelectric materials. Cole-Cole plots indicate the polydispersive nature of the dielectric relaxation in $CaNb_2O_6$. AC conduction activation energies are estimated from Arrhenius plots and conduction mechanism is discussed.

Keywords: Crystal structure, X-ray techniques, Electrical properties.

1. INTRODUCTION

Microwave dielectrics such as $(Zr,Sn)TiO_4$, $Ba(Zn_{1/3}Ta_{2/3})O_3$ (BZT) and $Ba(Mg_{1/3}Ta_{2/3})O_3$ (BMT) oxide compounds have been widely investigated[1-3]. However, these oxides are needed high sintering temperature. Besides, Ta_2O_5 is an expensive

raw material as compared with Nb_2O_5. The columbite niobate compounds MNb_2O_6 (where M= Mg, Zn, Ni, Ca, Cu, Mn and Co) have received much attention due to low sintering temperature and low cost[4-7]. Recently, we have prepared $MgNb_2O_6$ in pure columbite phase[8]. Additionally, niobates have interesting photoactive and the luminescent properties[9-13]. The microwave dielectric properties of the columbites are to a large extent sensible to their preparation[14]. Moreover, the synthesis of single phase columbites is often difficult because of the formation of corundum-like crystal phases $A_4Nb_2O_9$[15]. The properties of ceramics are greatly affected by the characteristics of the powder such as particle size, morphology, purity and chemical composition. To best of our knowledge, all the reports mainly concerned with the preparation routes and detailed dielectric relaxation and electrical conduction mechanism are not studied. For any device application, an understanding of these properties is very much required along with a simple processing route.

We therefore, attempted the optimization of process parameters in simple solid state reaction route viz. rate of cooling and heating during calcination and sintering in order to prepare the $CaNb_2O_6$ (CN) in phase pure columbite structure keeping relatively low calcination temperature. Synthesis, dielectric and electrical conductivity of $CaNb_2O_6$ are investigated and presented in the paper.

2. EXPERIMENTAL PROCEDURE

$CaNb_2O_6$ is synthesized by taking stoichiometric amounts of $CaCO_3$ (Loba Chem. 99.9%), Nb_2O_5 (Loba Chem. 99.5%) using solid-state reaction route. The stoichiometric amounts of constituent's powders were wet mixed in acetone for 6 hours. The mixed powders were calcined at 1200^oC for 6 hours at the rate of 2^0C/m. Calcined powders were structurally analyzed using X-ray diffraction data which were carried out using X-ray diffractometer (Rigaku, Miniflex) with Cu K_α λ=1.54056 *Å*. Fine calcined powders were pressed into cylindrical pellets of 10 mm diameter and 1-2 mm thickness under an isostatic pressure of 100 MPa. Polyvinyl alcohol (PVA) was used as a binder. The pellet were sintered at 1250^0C for 6 hours and cooled down to room temperature using controlled cooling rate 2^0C/m. Prepared compounds were used for dielectric, and electrical conductivity measurement. The phase formation of the sintered pellet has been identified using X-ray diffraction analysis again**.** To determine the dielectric properties, the sintered samples were electroded with silver paste and heated at 300^0C for 2 hour before measurements were performed. The electrical measurements were performed at various temperatures, using a computer controlled LCR HI-TESTER (HIOKI-3532-50). The microstruc-ture and grain size distribution of the sintered pellets were studied by scanning electron micrograph using JEOL JSM-5800 Scanning electron microscope at 20 kV.

3. RESULT AND DISCUSSION

3.1 X-ray diffraction studies

Figure 1 Shows XRD pattern of $CaNb_2O_6$ sample calcined at 1200^0C, with the observed interplanar spacing (d_{obs}) of all the peaks of the XRD pattern, unit cell parameters were obtained using a standard computer software POWD [16]. The unit

cell with orthorhombic crystal system was selected for which $\Sigma\Delta d = \Sigma (d_{obs}-d_{cal})$ minimum. The 100% intensity peak was observed at $2\theta=29^0310'$ which was found to be the characteristic feature of the $CaNb_2O_6$. The major X-ray reflection peaks fitted satisfactorily in orthorhombic columbite phase with lattice constants $a=5.772A^0$ $b=14.9897A^0$, $c=5.2375A^0$ which is so close to earlier report (JCPDS No.11 -0619) of a=5.764, b=15.09, c=5.232.

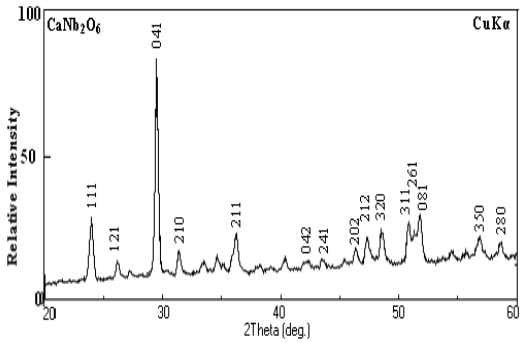

Figure: 1 X-RD pattern of pure phase $CaNb_2O_6$ calcined at 1200^0C

Density of material were found to be 4.36 g_m/cm^3 (92% of theoretical density), in the sample sintered at 1250^0C. The microstructure of the sintered pellets and distribution of grains over the sample surface were studied by scanning electron micrographs. The typical SEM micrograph of $CaNb_2O_6$ is shown in inset of Fig.1. Although CN stabilize in pure phase but the grains are disc shaped and loosely packed. For complete grain growth apparently higher sintering temperature is required. The average grain size estimated by linear intercept method is found 1.2 μm at room temperature.

3.2 Dielectric Study

The temperature dependence of dielectric constant for $CaNb_2O_6$ at different frequencies is shown in Fig.2 and the corresponding dielectric losses are shown in the inset of the Fig.2. The value of dielectric constant (ε') increases with increase in temperature and a peak evolves at 112^0C (ε_m = 24 at 0.5 kHz).

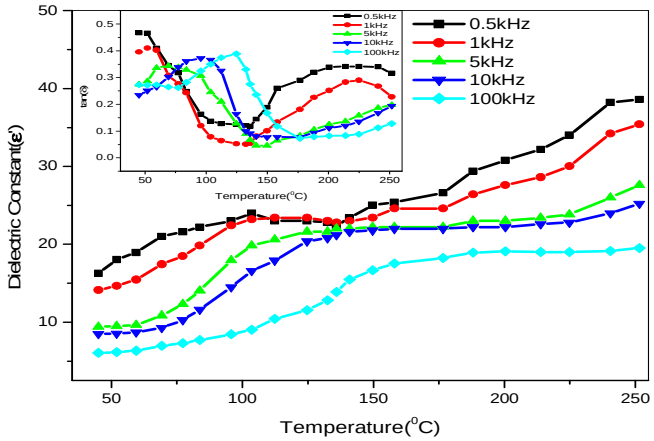

Figure:2 Temperature dependence of dielectric constant (ε'). Inset shows corresponding temperature dependence tangent loss.

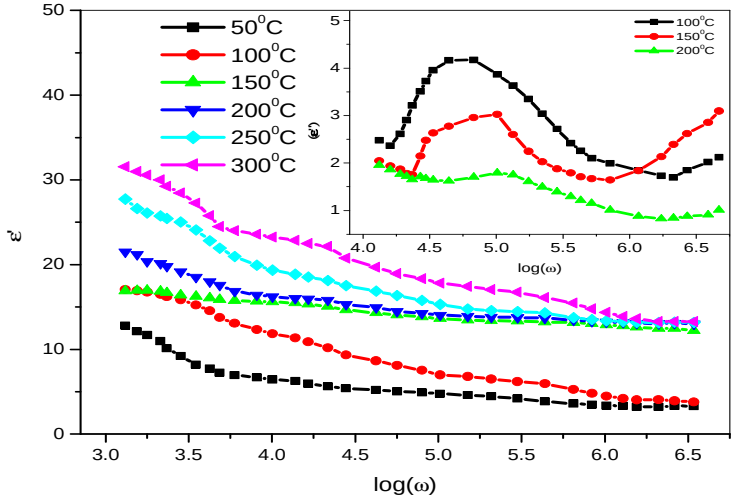

Figure: 3 Frequency dependence of real ε' part of dielectric constant. Inset shows frequency dependence of imaginary ε'' part of dielectric constant.

Although CN shows very low dielectric constant response, the behaviour of the material is not clearly understood furthermore, it has very peculiar properties like as materials having diffused dielectric response may due to conducting domain wall. Both ε' and tan (δ) shows a broad maximum value of ε' (ε_{max}), which decreases with increase in frequency. Dielectric loss increases sharply and then decreases with further increase in temperature. The kind of temperature dependence of the loss is typically associated with losses by conduction. Frequency dependence of dielectric constant shown in Fig. 3 and corresponding loss is shown in inset of Fig. 3. A general feature of the dielectric response is that dielectric constant values decrease with increasing the frequency of excitation and the high frequency dielectric behavior becomes temperature independent. Dielectric loss shows peak, which varies with temperature. The value of (ε') at lower frequencies in general, increases with decreasing frequency and increasing temperature. This may be attributed to be free charge buildup at the interface between the sample and the electrode (space charge polarization). In order to understand the diffusion processes operating the system, the Cole-Cole formalism is adopted for analyzing the frequency dependence of dielectric response.

The Debye equation is modified in order to introduce diffuseness parameter as[17]

$$\varepsilon^* = \varepsilon' - j\varepsilon'' = \varepsilon_\infty + \frac{(\varepsilon_s - \varepsilon_\infty)}{(1 + j\omega\tau)^{1-\alpha}} \qquad (1)$$

from this equation one can get the equation of circle as

$$\left(\varepsilon'' + \frac{1}{2}(\varepsilon_s - \varepsilon_\infty)tan\alpha\pi/2\right)^2 + \left(\varepsilon' - \frac{1}{2}(\varepsilon_s - \varepsilon_\infty)\right)^2 = \left(\frac{1}{2}\ (\varepsilon_s - \varepsilon_\infty)sec\alpha/2\right)^2 \qquad (2)$$

where ε_s and ε_∞ are the low and high frequency values of ε' , α is a measure of

the distribution of relaxation times, $\tau = \omega^{-1}$. The parameter, α can be determined from the location of the center of the Cole-Cole circles, of which only an arc lies above the ε' axis. Such plots are shown in Figure 4.

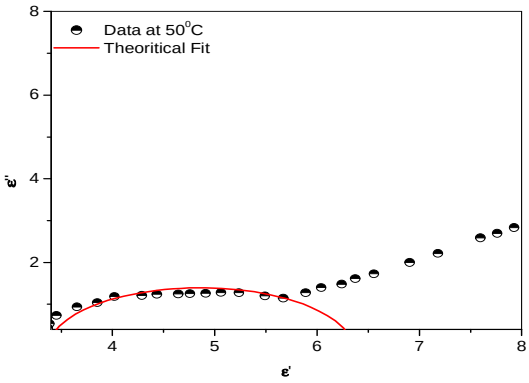

Figure: 4 Cole-Cole plot between (ε') and (ε'').

It is evident from these plots that the relaxation process differs from the Debye process (for which α=0). The parameter, α as determined from the angle subtended by the radius of the circle with the real axis passing through the origin of ε'–axis, has the value α =0.11. Thus the Cole-Cole plots indicate the polydispersive nature of the dielectric relaxation in $CaNb_2O_6$.

3.3 AC Electrical Conductivity Study

The ac conductivity was calculated from the impedance data using the relation $\sigma_{ac} = \omega\varepsilon_0\varepsilon_r (\tan\delta)$. It is clear from the figure that the material at low frequencies exhibits dispersion. Conductivity increases with increase in temperature and frequency. The conductivity could be fitted through the expression $\sigma_{ac} = \sigma_{dc} + A\omega^n$, known as Jonsher's law[18], where A is a thermally activated quantity and n is the frequency dependent exponent that takes values < 1. The data were fitted using the above relation and the calculated values of σ_{dc}, A and n are shown in table 1. The best fit of frequency dependent ac conductivity shown in Fig. 5.

This indicates that the conduction process is a thermally activated phenomenon.

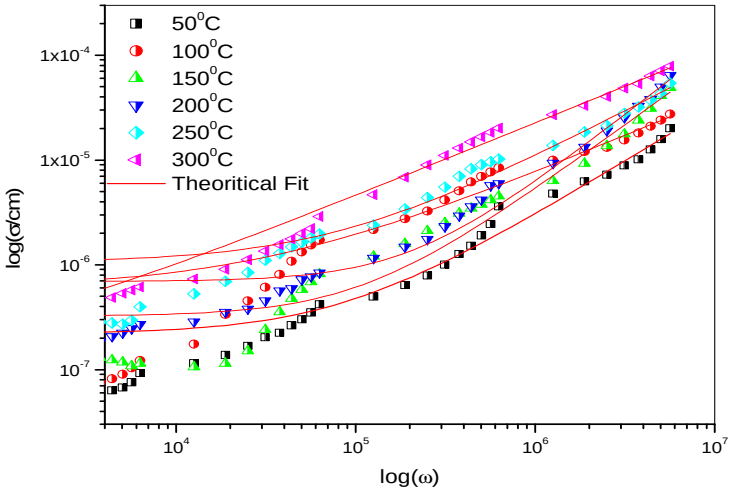

Figure: 5 A.C conductivity plotted as function of (logω) for $CaNb_2O_6$.

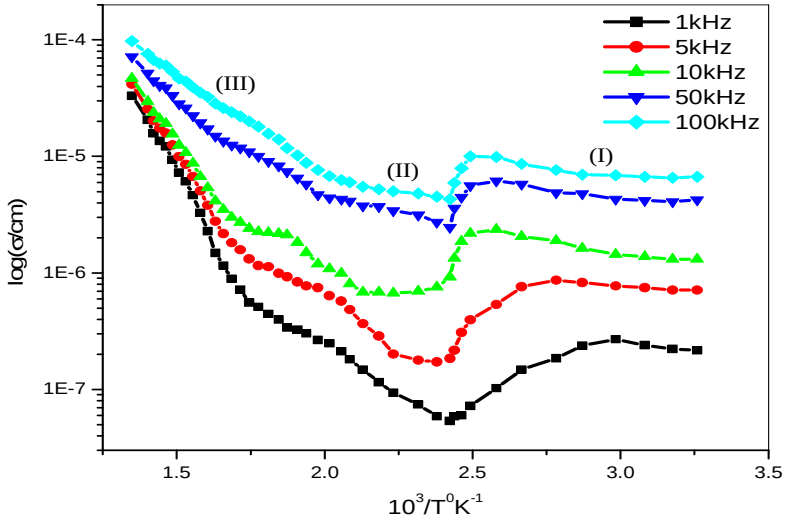

Figure: 6 Temperature dependence of AC conductivity at different frequencies for $CaNb_2O_6$.

Table: 1Non-linear fitting data from equation $\sigma_{ac} = \sigma_{dc} + A\omega^n$.

Temperature(^{0}C)	σ_{dc}	A	n
50	2.2×10^{-7}	1.5×10^{-12}	0.94
100	5.9×10^{-7}	3.3×10^{-12}	0.97
150	6.2×10^{-7}	1.6×10^{-13}	1.00
200	6.9×10^{-7}	4.9×10^{-14}	0.99
250	1.0×10^{-6}	4.2×10^{-11}	0.89
300	1.2×10^{-6}	1.5×10^{-9}	0.69

According to Jonsher, the origin of the frequency dependent conductivity lies in the relaxation phenomenon arising due to mobile charge carriers. The low frequency dispersion thus is associated with ac conductivity whereas almost frequency independent (especially at higher temperatures) conductivity at high frequencies corresponds to the dc conductivity of the material. The temperature at which the grain resistance dominates over grain boundary is marked by change in slope of conductivity with frequency. The frequency at which the slope changes is known as hopping frequency, which corresponds to polaron hopping of charges species. The oxygen vacancies may act as polaron[19]. As the temperature increases, the hopping frequency shifts towards lower side. The charged species that are freed from grains are trapped into grain boundaries. Temperature dependence of ac conductivity of material is shown in figure 6. The change in slope of conductivity plots (Fig. 6) suggests that, it can be divided into three regions, which are (i) 50-140^{0}C, (ii) 150-280^{0}C and (iii) 290-450^{0}C.

The conductivity of the material is

found to independent from temperature (at lower temperature), independent part of curve increases with increase in frequency. As the frequency decreases, oxygen vacancies and other defects become active hence no anomalies appeared in region three. Also the main contribution to the conductivity in this region may result from space charge. As temperature increases, space charges are released[20] and recombined and hence curves almost merge at region three.

Table:2 Activation energies values at different frequencies calculated by linear fitting of temperature dependence of AC conductivity for BN at given range of temperature.

Frequency in (kHz)	Temperature Range		
	Activation Energy (eV) 30^0C to 100^0C	Activation Energy (eV) 150^0C to 280^0C	Activation Energy (eV) 290^0C to 450^0C
1	0.03	0.13	0.33
5	0.02	0.12	0.33
10	0.03	0.08	0.28
50	0.02	0.07	0.17
100	0.02	0.07	0.14

The activation energy values in the system have been calculated from the slope of the graph (Fig.6) for three regions and are given in table 2.

4. CONCLUSIONS

Phase pure columbite structure in $CaNb_2O_6$ is stabilized through standard solid state reaction route by using controlled cooling rate during calcination and sintering. The crystal structure is orthorhombic with unit cell parameter a=5.772Å b=14.9897Å, c=5.2375Å. The experimental density is >92% and average grain size is 1.2 μm. Temperature dependent of ε' and ε'' shows that the compound exhibit dielectric anomaly at 112^0C, indicating that the dielectric polarization has a relaxation type behavior. Cole-Cole plots indicate the polydispersive nature of the dielectric relaxation in $CaNb_2O_6$. AC conductivity exhibits dispersion at low frequencies and follows Jonscher's power law. The charge in the exponent n in ac conductivity dispersion term ($A\omega^n$) shows that the nature of conductivity mechanics. Charges from localized hopping to free ion motion with increase in temperature and that the conduction is a thermally activated process.

REFERENCES

1. K. Wakino, T. Minai, H. Tamura, *J. Am. Ceram. Soc*. 67, 278 (1984).
2. S. Kawashima, M. Nishida, I. Ueda, H. Ouchi, *J. Am. Ceram. Soc*. 66 (6), 233 (1983).
3. K. Matsumoto, T. Hiuga, K. Takada, H. Ichimura, *IEEE Trans. Ultrason. Ferroelec. Freq. Contr*. 33 (6) 802 (1986).

4. M. Meada, T. Yamamura, T. Ikeda, *Jpn. J. Appl. Phys. Supp*. 26-2, 76 (1987).
5. H.J. Lee, I.T. Kim, K.S. Hong, *Jpn. J. Appl. Phys.,* Part 2 36 (10A), 1318 (1997).
6. H.J. Lee, K.J. Hong, S.J. Kim, I.T. Kim, *Mater. Res. Bull*. 32 (7), 847 (1997).
7. C.S. Hsu, C.L. Huang, J.F. Tseng, C.Y. Huang, *Mater. Res. Bull*. 38, 1091 (2003).
8. K.N.Singh and P.K. Bajpai, Physica B, *Condensed Matter*, 405, 303 (2010).
9. D. Hreniak, A. Speghini, M. Bettinelli, W. Strek, *J. Lumin.* 219, 119 (2006).
10. T.H. Fang, Y.J. Hsiao, Y.S. Chang, Y.H. Chang, *Mater. Chem. Phys*. 100, 418 (2006).
11. X.Z. Xiao, B. Yan, *J. Alloys Compd*. 421, 252 (2006).
12. Y.J. Hsiao, T.H. Fang, Y.S. Chang, Y.H. Chang, C.H. Liu, L.W. Ji, W.Y. Jywe, *J. Lumin.*126, 866 (2007).
13. G. Zhang, F. Hea, X. Zoua, J. Gonga, H. Tu, H. Zhang, Q. Zhang, Y. Liu, *J. Alloys Compd*. 427, 82 (2007).
14. R. C. Pullar, , J. D. Breeze and N. Mc. N. Alford, , *J. Am. Ceram. Soc.*, 88: 9, 2466 (2005).
15. A. Ananta, , R. Brydson, and N. W. Thomas, *J. Eur. Ceram.Soc.*,19:3, 355 (1999).
16. E. Wu, "POWD", an Interactive Powder Diffraction Data Interpretation and Indexing Programme, *Ver. 2.1*, School of Physical Sciences, Flinders University of South Australia, Bedford Park, S.A.,5042,Australia.
17. K.S. Cole, R.H. Cole, *J. Chem. Phys*. 9: 341 (1941).
18. A.K. Jonscher, *J. Mat. Sc*, 16, 2037 (1981).
19. C. Ang, Z.Ye, L.E. Cross, *Phys. Rev.* B 62, 228 (2000).
20. T. R. Shrout, H. Chenand, L. E. Cross, *Ferroelectric letters*, 74, 317 (1987).